AD-A152 707 A SIMPLE PHENOMENOLOGICAL MODEL FOR THE INTERPRETATION OF ION NEUTRALIZATION SPECTRA(U) CALIFORNIA UNIV SANTA BARBARA DEPT OF CHEMISTRY E HOOD ET AL. NOV 83 TR-12 1/1

UNCLASSIFIED N00014-81-K-0598 F/G 20/8 NL

END

FILMED

DTIC

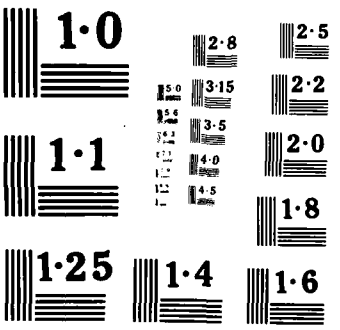
1·0
2·8
2·5
3·15
2·2
3·5
1·1
4·0
2·0
4·5
1·8
1·25
1·4
1·6

(2)

REPORT DOCUMENTATION PAGE		READ INSTRUCTIONS BEFORE COMPLETING FORM
1. REPORT NUMBER: 12	2. GOVT ACCESSION NO.	3. RECIPIENT'S CATALOG NUMBER
4. TITLE (and Subtitle): A SIMPLE PHENOMENOLOGICAL MODEL FOR THE INTERPRETATION OF ION NEUTRALIZATION SPECTRA		5. TYPE OF REPORT & PERIOD COVERED: Annual Technical Report 6. PERFORMING ORG. REPORT NUMBER
7. AUTHOR(s): Eric Hood, Ferenc Bozso and Horia Metiu		8. CONTRACT OR GRANT NUMBER(s): N00014-81-K-0598
9. PERFORMING ORGANIZATION NAME AND ADDRESS: University of California, Department of Chemistry, Santa Barbara, Ca. 93106		10. PROGRAM ELEMENT, PROJECT, TASK AREA & WORK UNIT NUMBERS: NR 056-766/4-21/81 (472)
11. CONTROLLING OFFICE NAME AND ADDRESS: Office of Naval Research, Department of the Navy, Code: 612A: DKB, Arlington, VA 22217		12. REPORT DATE: November 1983 13. NUMBER OF PAGES: 40
14. MONITORING AGENCY NAME & ADDRESS (if different from Controlling Office): Office of Naval Research Detachment Pasadena, 1030 East Green Street, Pasadena, CA 91105		15. SECURITY CLASS. (of this report): unclassified/unlimited 15a. DECLASSIFICATION/DOWNGRADING SCHEDULE

16. DISTRIBUTION STATEMENT (of this Report)

This document has been approved for public release and sale; its distribution is unlimited.

17. DISTRIBUTION STATEMENT (of the abstract entered in Block 20, if different from Report)

18. SUPPLEMENTARY NOTES

Submitted to Surface Science

19. KEY WORDS (Continue on reverse side if necessary and identify by block number)

20. ABSTRACT (Continue on reverse side if necessary and identify by block number)

We present here an extention of Hagstrum's model for the interpretation of ion neutralization spectra. We take into account the fact that the neutralization process depends on both the density of states and the orbital size and takes place continuously at all surface-ion seperation distances at which the ion and metal orbitals overlap. The model is applied to the calculation of the density of states of the Ni(111) surface.

OFFICE OF NAVAL RESEARCH

Contract N00014-81-K-0598

Task No. NR 056-766/4-21-81 (472)

Technical Report No. 12

A SIMPLE PHENOMENOLOGICAL MODEL FOR THE INTERPRETATION OF ION NEUTRALIZATION SPECTRA

by

E. Hood, F. Bozco and H. Metiu

Submitted to SURFACE SCIENCE (1985)

University of California
Department of Chemistry
Santa Barbara, CA 93106

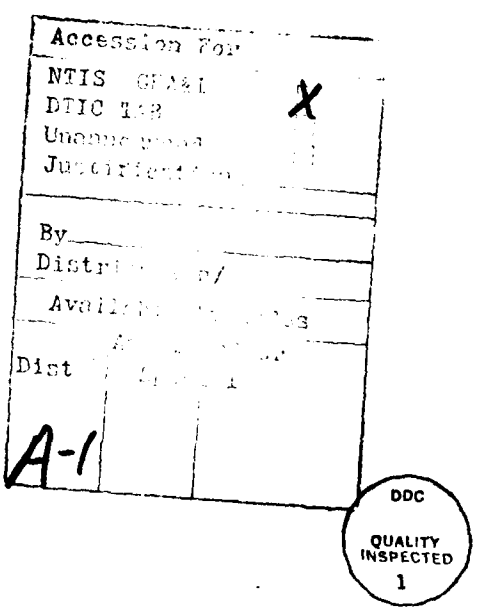

A SIMPLE PHENOMENOLOGICAL MODEL FOR THE INTERPRETATION OF ION NEUTRALIZATION SPECTRA

Eric Hood[a]
Noyes Laboratory of Chemical Physics
California Institute of Technology
Pasadena, California 91106

Ferenc Bozso
Department of Chemistry
Pittsburgh University
Pittsburgh, PA 15260

Horia Metiu[b]
Department of Chemistry
University of California
Santa Barbara, California 93106

(a) Work performed as a graduate student at UC Santa Barbara. Ph.D. Thesis submitted to UC Santa Barbara in November 1983.

(b) Camille and Henry Dreyfus Teacher-Scholar

ABSTRACT

We present here an extension of Hagstrum's model for the interpretation of ion neutralization spectra. We take into account the fact that the neutralization process depends on both the density of states and the orbital size and takes place continuously at all surface-ion separation distances at which the ion and metal orbitals overlap. The model is applied to the calculation of the density of states of the Ni(111) surface.

I. INTRODUCTION

It has been demonstrated by Hagstrum that ion neutralization can be used to probe the outermost layer of a solid surface.[1-4] This is experimentally achieved by exposing the surface to a low kinetic energy (10-100 eV) ion beam. The ions are neutralized by a two electron Auger process, which causes electron ejection from the surface. The kinetic energy of the ejected electrons contains information about the electronic states of the surface.

The development of metastable quenching spectroscopy[5-7] has increased the interest in ion neutralization spectroscopy by extending it to very low (i.e. ~0.05 eV) incident kinetic energies. This technique exposes the surface to a thermal beam containing ground state and metastable noble gas atoms. Under certain conditions (i.e. when the work function of the surface is larger or only slightly lower than the ionization potential of the metastable) the impinging metastable is ionized by resonant charge transfer to the surface. The resulting noble gas ion collides with the surface and generates an ion neutralization spectrum.

The interpretation of IN spectra is based on a simple model proposed by Hagstrum,[2,4] which expresses the spectrum in terms of a convolution of the electronic density of states with itself. In certain cases it is necessary to extend this model to include the matrix elements of the Auger neutralization process and the motion of the incident ion. In this paper we provide such an extension, which is simple enough to be a practical tool for the interpretation of the IN spectra. The model could also be useful in the analysis of other surface science techniques in which ion neutralization plays a part: electron stimulated desorption (ESD),[8] electron stimulated desorption ion angular distribution (ESDIAD),[9] secondary ion mass spectroscopy (SIMS)[10] and others.[11]

II. THE MODEL DESCRIBING THE AUGER NEUTRALIZATION PROCESS.

II. 1. The Curve Crossing Description.

The Auger process is simply described by the curve crossing model explained below. The orbitals involved in the Auger transition are shown in Figure 1: ψ_i is the singly occupied orbital of the impinging ion, ψ_μ and ψ_ν are the orbitals containing the two metal electrons involved in the transition, and ψ_k is the metal orbital (located above the vacuum) to which the ejected electron is promoted. In the initial state (Figure 1a) there is a hole in ψ_i and ψ_k is empty. In the final state ψ_μ and ψ_ν have a hole and ψ_i and ψ_k are doubly and singly populated, respectively

To describe the energetics of this system we use the energy of the ground state metal plus that of the neutral atom at infinite distance from the surface, as a zero energy reference. Within the one electron picture discussed above the initial state energy is $\varepsilon_i(z)$, and the final state energy is $\varepsilon_\mu + \varepsilon_\nu + \varepsilon_k + V(z)$. Here $V(z)$ is the energy of interaction between the neutral and the ionized surface when they are separated by a distance z, and ε_j is the energy of the orbital ψ_j.

The energy conservation condition for an Auger process taking place when the ion is at a distance z from the surface is

$$\varepsilon_k + \varepsilon_\mu + \varepsilon_\nu + V(z) = \varepsilon_i(z) \quad . \tag{1}$$

We note that it is not necessary to use the one-electron energies to describe this system. The quantity $\varepsilon_i(z) - V(z) \equiv I(z)$ can be replaced by the ionization energy of the atom located at the distance z from the surface; $\varepsilon_\mu + \varepsilon_\nu + \varepsilon_k$ can be replaced by the total energy of the excited, positively charged metal surface (denoted $(Me^+)^*_{\mu\nu k}$) created by the Auger neutralization.

The dependence of the initial and final state energies on the particle surface distance is schematically plotted in Figure 2. The upper curve, called in what follows the ionic curve, represents the interaction energy

of the metal-ion system ($Me+A^+$), which is dominated by the image force at longer distances and is repulsive at shorter ones. The lower curve, called in what follows the neutral curve, is the energy of the neutral atom interacting with $(Me^+)^*_{\mu\nu k}$. The neutral curve has a much weaker distance dependence than the ionic one.

The separation between the curves, called here the energy mismatch, is

$$\Delta_{k,\alpha}(z) = I(z)-\varepsilon_k-\alpha \quad . \tag{2}$$

We introduce the notation $\alpha = \varepsilon_\mu+\varepsilon_\nu$ since the energy mismatch depends on α only, not on ε_μ and ε_ν separately.

If we assume that the interaction energy between the atom and $(Me^+)^*_{\mu\nu k}$ is independent of ε_μ and ε_ν (at fixed ε_k), then the neutral curve is highly degenerate: there are,

$$N_{k,\alpha} = \int d\varepsilon_\mu \int d\varepsilon_\nu \rho(\varepsilon_\mu)\rho(\varepsilon_\nu)\ \delta(\varepsilon_\mu+\varepsilon_\nu-\alpha)$$

states having different ε_μ and ε_ν, but the same α. One of the models proposed by Hagstrum[4] assumes that the Auger process takes place at fix $\alpha=\alpha_0$ and the number of Auger electrons having energy ε_k is proportional to N_{k,α_0}. Deconvolution of the Auger spectrum can therefore provide the density of states $\rho(\varepsilon)$.

If we consider two values of α, namely α' and α'' (and fix ε_k), we generate two neutral curves as shown in Figure 3. These curves have different asymptotic energy mismatches $\Delta_{k,\alpha'}(\infty)$ and $\Delta_{k,\alpha''}(\infty)$ equal to $I(\infty)-\alpha'-\varepsilon_k$ and $I(\infty)-\alpha''-\varepsilon_k$, respectively. They cross the ionic curve at two different points $Z(\alpha')$ and $Z(\alpha'')$, which can be obtained by solving the equation

$$\Delta_{k,\alpha}(Z(\alpha)) = I(Z(\alpha))-\varepsilon_k-\alpha=0 \tag{3}$$

for $\alpha=\alpha'$ and $\alpha=\alpha''$.

Since the Auger neutralization process, generating an Auger electron with kinetic energy ε_k, can take place for all the neutral curves that cross the ionic one (i.e. for which the equation $\Delta_{k,\alpha}(z)=0$ has a solution) we must, in principle, consider the whole family of neutral curves labelled by α. Thus the ionic curve interacts with a continuous band of neutral curves, which are schematically drawn in Figure 4.

II. 2. The ionization rate.

The simplest model for the computation of the rate of production of an electron with energy ε_k uses the Golden Rule formula

$$W_k(\alpha) = (2\pi/\hbar) \int d\varepsilon_\mu \int d\varepsilon_\nu \, |H(\varepsilon_k,\varepsilon_\mu,\varepsilon_\nu;Z(\alpha))|^2 \, \rho(\varepsilon_\mu)\rho(\varepsilon_\nu)\rho(\varepsilon_k) \\ \delta(I_\alpha-\varepsilon_\mu-\varepsilon_\nu-\varepsilon_k) \, \delta(\alpha-\varepsilon_\mu-\varepsilon_\nu) \tag{4}$$

We consider here only one neutral curve α, which crosses the ionic curve at $z=Z(\alpha)$, where the ionization potential is $I_\alpha=I(Z(\alpha))$. One of the δ-functions in Equation (4) keeps only those values of ε_μ and ε_ν that add up to α; the other enforces the energy conservation specified by Equation (1). The matrix element $H(\varepsilon_k,\varepsilon_\mu,\varepsilon_\nu;Z(\alpha))$, for which we use the notation H when an explicit designation of the variables is not necessary, will be discussed in Section II.3.

As the ion approaches the surface on the trajectory $z=z(t)$, it passes through various crossing points $Z(\alpha)$, corresponding to various values of α. By using $z(t)=Z(\alpha)$, where $Z(\alpha)$ is the crossing point for curve α, we can find the function $\alpha(t)$ giving the curve being crossed at time t. The probability $P_\kappa(t)$ that an electron of kinetic energy ε_κ is produced at time t (i.e. at the position $z(t)=Z(\alpha)$ where the curve $\alpha(t)$ is crossed) is given by

$$P_k(t) = p(z(t))\mathcal{P}_k \, W_k(\alpha(t)) \quad ; \tag{5}$$

where $p(z(t))$ is the probability that the ion reached the point z(t) without being neutralized, $\mathcal{P}_k$ is the probability that the Auger electron escapes into

the vacuum, and $W_k(\alpha(t))$ is the rate of electron production given by Equation (4).

The survival probability p(z(t) is given by the rate equation

$$\frac{dpz(t)}{dt} = -W(\alpha(t))\, pz(t)) \tag{6}$$

where

$$W(\alpha) = \int d\varepsilon_k W_k(\alpha) \quad . \tag{7}$$

Assuming that we know the trajectory of the ion we can write the finite difference version of Equation (6) as

$$p(z_{i+1}) - p(z_i) = -W(\alpha_i)p(z_i)v_i^{-1}(z_{i+1}-z_i) \tag{8}$$

where $z_i = z(t_i)$, $\alpha_i \equiv \alpha(t_i)$, $v_i = dz/dt|_{t=t_i}$, and the points t_i form a fine grid on the time axis.

The above equations provide a computational scheme for the probability of generating an electron with kinetic energy ε_k, after the incident particle has completed its trajectory. To start, we must provide an equation of motion

$$md^2z/dt^2 = F(z) \tag{9}$$

to propagate the ion and generate its trajectory. The force F(z) is discussed in Section II.4.

To compute $W(\alpha_i)$, which is needed in Equation (8), we must make a model for $H(\varepsilon_k,\varepsilon_\mu,\varepsilon_\nu;z_i)$, use it in Equation (4) to compute $W_k(\alpha_i)$, which is then used in Equation (7) to compute $W(\alpha_i)$. We can now solve Equation (8) to obtain the survival probability $p(t_i)$, then use an empirical formula for the escape probability $\mathcal{P}_k$, and calculate, from Equation (5), the probability $P_k(t_i)$ that an electron of energy ε_k is generated at t_i. Adding up over all the times,

$$N_k = \sum_i P(t_i) \quad , \tag{10}$$

we obtain the probability N_k that an ion generates an electron of kinetic energy ε_k. This is the computed IN spectrum, which can be compared to the

experimental results (after removing from the measured spectrum the contribution form the secondary electron emission) to determine either the density of states that best fits the data (if one has a reasonable model for the matrix element H) or to get the matrix element (if the density of states is known).

II. 3. The relationship to previous work.

Since the present work is an extension of that of Hagstrum it is useful to show explicitly the connection to his model. To do this we must make several approximations. First we assume that the rate of electron production is dominated by one of the curves of the family labelled by α, namely that corresponding to $\alpha=\alpha_o$. This reduces the problem to a single curve crossing (Figure 2). This approximation is reasonable only if $W_k(\alpha)$ is very small for all $\alpha<\alpha_o$ and has a large increase at α_o, such that the probability of having been neutralized for $z>Z(\alpha_o)$, and the probability having survived as an ion for $z<Z(\alpha_o)$, are both minimal.

Under these conditions the rate W_k^H of production of an electron of energy ε_k is proportional to

$$W_k^H \propto \rho(\varepsilon_k) \int d\varepsilon_\mu \int d\varepsilon_\nu \; |H|^2 \; \rho(\varepsilon_\mu)\rho(\varepsilon_\nu) \; \delta(I_{\alpha_o}-\varepsilon_\mu-\varepsilon_\nu-\varepsilon_k) \; \delta(\alpha_o-\varepsilon_\mu-\varepsilon_\nu) \quad (11)$$

where α_o is the only value of α which we need to consider.

If we assume that $\rho(\varepsilon_k)$ is independent of ε_k and that $H(\varepsilon_k,\varepsilon_\mu,\varepsilon_\nu;Z(\alpha_o))$ is independent of $\varepsilon_\mu,\varepsilon_\nu$ and ε_k we can write that W_k^H is proportional to

$$W_k^H \propto \int d\beta \; \rho(E_k+\beta)\rho(E_k-\beta) \quad (12)$$

with

$$E_k = (I(Z(\alpha_o)) - \varepsilon_k)/2 \quad (13)$$

Thus the IN spectrum generated by this model is the convolution of the density of states with itself; the use of a deconvolution program can supply $\rho(\varepsilon)$, if W_k^H is measured. If $|H|^2$ and $\rho(\varepsilon_k)$ depend strongly on $\varepsilon_\mu,\varepsilon_\nu$ and ε_k we can define

$$\bar{o}(\varepsilon) \equiv |H|\, o(\varepsilon_k)^{1/2}\, \rho(\varepsilon) \tag{14}$$

and use

$$W_k^H \propto \int \bar{\rho}(E_k+\beta)\, \bar{o}(E_k-\beta)d\beta \tag{15}$$

Clearly Equation (15) is less useful than Equation (12) since it provides only the product of various quantities which are of interest individually.

II. 4. The model for the matrix elements.

The assumption made in Hagstrum model that the matrix element H is independent on ε_μ and ε_ν is likely to be inadequate, the nature of the surface orbitals changes with the orbital energy. Consider, for example, the case of a metal that has two bands A and B: A is narrow and its energy is larger than that of broad band B; furthermore, the orbitals of A are localized tightly around the metal atoms, while those of B reach further in space. (This is consistent with the fact that the band A is narrower than B). Such a situation appears in the case of Ni, for example, where the 3d band corresponds to band A and the s-p band to B, and the 3d orbital are much tighter than the s ones.

If we were to apply Hagstrum model to this system we need to consider two distances, Z_A and Z_B, corresponding to the distances at which the band A or B, respectively, neutralizes most efficiently the hole in the incident ion. Since the orbitals of band B reach further in vacuum than those of A, the distance Z_B is larger than Z_A. As the ion approaches the surface it will first reach Z_B and the Auger neutralization can occur by electron transfer from B to the ion and electron ejection from either B or A. We denote these processes as BB and BA, respectively. The surviving ions can then reach Z_A and be Auger neutralized by electron transfer from A to the ion and electron ejection from either A or B (processess AA and AB).

The shape of the IN spectrum is influenced by the difference in the spatial properties of the orbitals. At the distance Z_B the BB process generates electrons in the kinetic energy range (See Figure 5).

$$I(Z_B) - 2\varepsilon_1 \leq \varepsilon_k \leq I(Z_B) - 2\varepsilon_2$$

and AB in the range

$$I(Z_B) - \varepsilon_1 - \varepsilon_2 \leq \varepsilon_k \leq I(Z_B) - \varepsilon_2 - \varepsilon_F \quad .$$

At the distance Z_A the kinetic energy of the ejected electrons is in the range

$$I(Z_A) - 2\varepsilon_2 < \varepsilon_k < I(Z_A) - 2\varepsilon_F$$

for AA, and

$$I(Z_A) - \varepsilon_2 - \varepsilon_1 < \varepsilon_k < I(Z_A) - \varepsilon_F - \varepsilon_2$$

for BA. These ranges are schematically shown in Figure 5.

If, for example, the density of states of the B band is very high (and much higher than that of A) we expect BB to be very efficient and AB moderately efficient. Furthermore, most of the ions are neutralized at Z_B and very few reach Z_A. For those that do, neutralization by the BA process is more efficient than AA. The resulting IN spectrum having a very intense BB emission, a weak AB one, and an even weaker BA one, is schematically displayed in Figure 7 as a full line. If, for example, the band A reaches far in space and has a high density of states, the spectrum is dominated by the AA process, has a weak BA component and an even weaker AB. The resulting spectrum is shown schematically by the dotted lines in Figure 7. Clearly the shape of the spectrum is affected by <u>both the density of states and the spatial extent</u> of the orbitals forming the bands. The latter element is missing in the Hagstrum model.

A quantitative evaluation of the Auger matrix elements is very difficult since the relevant electronic wave functions are those of the surface in the presence of the neutral or the ion. For this reason we intend to pursue the

$$H_{fi}(z) = \frac{(2\pi)^2 \overline{C}}{\lambda(\alpha_\nu - \lambda)} e^{-(\lambda-\alpha_\mu)z} \int_0^{z-\gamma} d\omega \left\{ \frac{\omega e^{-(\beta-\alpha_\mu-\lambda)\omega}}{\beta} - \frac{e^{-(\beta-\alpha_\mu-\lambda)\omega}}{\beta^2} \right\} \quad \text{for } \beta > 0 \quad . \tag{A17}$$

Integration of Eq. (A17) gives the following formula for the INS matrix element for an incident ion at a separation distance z from the metallic surface plane

$$-H_{fi}(z) = \frac{(2\pi)^2 C_i C_k C_\nu C_\mu}{\lambda(\alpha_\nu - \lambda)\beta(\beta-\alpha_\mu-\lambda)} \left\{ e^{-\beta(z-\gamma)} e^{-(\alpha_\mu-\lambda)\gamma} \left[(z-\gamma) - \frac{1}{(\beta-\alpha_\mu-\lambda)} - \frac{1}{\beta} \right] - e^{-(\alpha_\mu-\lambda)z} \left[\frac{1}{(\beta-\alpha_\mu-\lambda)} - \frac{1}{\beta} \right] \right\} \tag{A18}$$

for $\alpha_\nu > \lambda > 0$, $\beta > (\alpha_\mu - \lambda) > 0$, and $z > \gamma$.

$$H_{fi}(z) = \frac{(2\pi)^2 \overline{C}}{\lambda(\alpha_\nu - \lambda)} \int_0^{z-\gamma} d\omega e^{-\alpha_\mu (z-\omega)} \int_0^{\infty} \tilde{\rho} d\tilde{\rho} e^{-\beta(\tilde{\rho}^2 - \omega^2)^{1/2}} e^{-\lambda(z-\omega)}$$

$$\text{for } \alpha_\nu > \lambda > 0 \ . \qquad \text{(A13)}$$

Now the focus of attention shifts to the integration over the variable $\tilde{\rho}$. We define the following variable transformation

$$t = \tilde{\rho}^2 \text{ and } g = (t+\omega^2)^{1/2} \ , \qquad \text{(A14a)}$$

and thus

$$dt = 2\tilde{\rho} d\tilde{\rho} \text{ and } dg = dt/[2(t+\omega^2)^{1/2}] \ , \qquad \text{(A14b)}$$

which gives

$$dt = 2gdg \ . \qquad \text{(A14c)}$$

Thus the integral over the variable $\tilde{\rho}$ becomes

$$\int_0^{\infty} d\tilde{\rho}\ \tilde{\rho}\ e^{-\beta(\tilde{\rho}^2 - \omega^2)^{1/2}} = \int_{\omega}^{\infty} dg\ g\ e^{-\beta g} \ . \qquad \text{(A15)}$$

Integration of Eq. (A15) by "parts" gives

$$\int_0^{\omega} dg\ g\ e^{-\beta g} = \frac{\omega e^{-\beta\omega}}{\beta} - \frac{e^{-\beta\omega}}{\beta^2} \quad \text{for } \beta > 0 \ . \qquad \text{(A16)}$$

Substituting the result of Eq. (A16) into Eq. (A13), we obtain the following integral expression for the INS matrix element

zero.

We begin to evaluate Eq. (A9) by concentrating on the integral over the variable ρ. We first define the following transformation of variables

$$\xi = (z-z'-\omega)^2 \text{ and } q = (\rho^2+\xi)^{1/2} , \tag{A10a}$$

and therefore

$$dq = \rho(\rho^2+\xi)^{-1/2}d\rho . \tag{A10b}$$

Through the use of Eq. (A10), the integral over the variable ρ becomes

$$\int_{\xi^{1/2}}^{\infty} dq\ e^{-\lambda q} = \frac{e^{-\lambda(z-z'-\omega)}}{\lambda} \text{ for } \lambda > 0. \tag{A11}$$

We proceed by evaluating the integral over the variable z' incorporating the result given in Eq. (A11)

$$\frac{e^{-\lambda(z-\omega)}}{\lambda} \int_0^{\infty} dz' e^{-(\alpha_y-\lambda)z'} = \frac{e^{-\lambda(z-\omega)}}{\lambda(\alpha_y-\lambda)} \text{ for } \alpha_y > \lambda > 0. \tag{A12}$$

Substituting Eqs. (A10) through (A12) into Eq. (A9), we obtain the following expression for the INS matrix element

metal surface completes the integration over the variable r_2 and gives the screened Coulomb interaction between the metallic conduction band wave function $\psi_\mu(r_1)$ and the ground state ion wave function $\psi_i(r_1)$ at the point Q with the metallic conduction band wave function $\psi_\nu(r_2)$ over the entire vacuum region

$$dV_Q = 2\pi\bar{C}e^{-\beta(\tilde{\rho}^2-\omega^2)^{1/2}} e^{-\alpha_\mu(z-\omega)} \int_0^\infty dz'\, e^{-\alpha_\nu z'} \times \int_0^\infty \frac{e^{-\lambda[\rho^2+(z-z'-\omega)^2]^{1/2}}}{[\rho^2+(z-z'-\omega)^2]^{1/2}} \rho d\rho \qquad (A8)$$

We now proceed with the integration over the variable r_1. We must contend with both the spherical geometry of the ion ground state wave function and the "planar" geometry of the metallic conduction band wave functions. Once again the cylindrical coordinate system is the system of choice. Thus the form of the integration over the variable r_1 is identical to the previously employed in the integration over the variable r_2. The integral expression for the INS matrix element thus becomes

$$H_{fi}(z) = (2\pi)^2\bar{C} \int_0^{z-\gamma} d\omega e^{-\alpha_\mu(z-\omega)} \int_0^\infty c\tilde{\rho} e^{-\beta(\tilde{\rho}^2-\omega^2)^{1/2}} d\tilde{\rho} \int_0^\infty dz' e^{-\alpha_\nu z'} \int_0^\infty \frac{e^{-\lambda[\rho^2+(z-z'-\omega)^2]^{1/2}}}{[\rho^2+(z-z'-\omega)^2]^{1/2}} \rho d\rho \qquad (A9)$$

where γ is introduced to truncate the integral as the separation distance between the ion core and the solid surface approaches

width $d\rho$ located on this $z = z'$ surface. The surface element contained within this annulus is $(2\pi\rho)d\rho$. All points residing within this annular surface element are equi-distant from the axial point Q. Thus the screened Coulomb interaction between the component of the metallic electronic wave function $\psi_\nu(r_2)$ contained within the annulus and the elements of the ground state ion wave function $\psi_i(r_1)$ and the metallic electronic wave function $\psi_\mu(r_1)$ at the point Q is given by

$$dV^{\alpha}_{z',Q} = \frac{\bar{C}e^{-\beta(\tilde{\rho}^2-\omega^2)^{1/2}}e^{-\lambda(\rho^2-z-z'-\omega)^2]^{1/2}}e^{-\alpha_\nu z'}e^{-\alpha_\mu(z-\omega)}2\pi\rho\cdot d\rho}{[\rho^2-(z-z'-\omega)^2]^{1/2}} \tag{A6}$$

Where $\bar{C}$ is defined $C_iC_kC_\nu C_\mu$. Since we approximate the wave function of the excited metallic electron to be constant over all space, its presence in the INS matrix element formula is denoted simply by C_k. The screened Coulomb interaction between the wave functions $\psi_i(r_1)$ and $\psi_\mu(r_1)$ at point Q and the metallic wave function $\psi_\nu(r_2)$ contained in the entire plane $z = z'$ is obtained by integrating Eq. (A6) over all the annuli of which the surface (x,y,z') is composed

$$dV_{z',Q} = 2\pi\bar{C}e^{-\alpha_\nu z'}e^{-\alpha_\mu(z-\omega)}e^{-\beta(\tilde{\rho}^2-\omega^2)^{1/2}}\int_0^\infty \frac{e^{-\lambda[\rho^2+(z-z'-\omega)^2]^{1/2}}}{[\rho^2-(z-z'-\omega)^2]^{1/2}}\rho d\rho \tag{A7}$$

Integration of Eq. (A7) over all possible planes parallel to the

Fig. 11. The wave function for the incident helium ion is an exponentially decaying function maximized at the position of the ionic nucleus .

$$\psi_i = C_i \exp(-\beta r) \quad . \tag{A3}$$

The electronic wave functions of the metallic conduction band have been modeled to decay exponentially in the vacuum region according to the following form $\psi_j = C_j \exp(-\alpha_j z)$ for $z > 0$. Thus points of equivalent metallic wave function amplitude form planes parallel to the surface of the semi-infinite metal slab. We focus on the plane located at $z = z'$. The amplitude of a metallic wave function at any point in the $(x,y,z = z')$ plane is denoted $\psi_j = C_j \exp(-\alpha_j z')$. The geometry associated with the metallic wave functions suggests the use of a cylindrical coordinate system. In this cylindrical coordinate system, the wave function for the incident helium ion becomes

$$\psi_i = C_i \exp[-\beta(\tilde{\rho}^2 - \omega^2)^{1/2}] \tag{A4}$$

while form of the metallic wave functions remain unchanged. Thus the screened Coulomb potential acquires the form

$$W(\vec{r}_1 - \vec{r}_2) = \exp(-\lambda[\rho^2-(z-z'-\omega)^2]^{1/2}) / [\rho^2-(z-z'-\omega)^2]^{1/2} \quad . \tag{A5}$$

We consider an infinitesimally thin annulus of radius ρ and

APPENDIX A:

An Outline of the Derivation of the INS Matrix Element

In order to evaluate the integrals appearing in Eq. (16) (and thus the matrix element associated with Auger neutralization), we consider a physical system composed of a semi-infinite metallic slab occupying the half-space (x,y,z<0) and an incident noble gas ion at the position (0,0,z).

The matrix element characterizing the Auger neutralization process is

$$H(\epsilon_k,\epsilon_\nu,\epsilon_\mu;z) = \int d\vec{r}_1 \int d\vec{r}_2\ \psi_i^*(\vec{r}_1)\psi_k^*(\vec{r}_2)W(\vec{r}_1-\vec{r}_2)\psi_\nu(\vec{r}_2)\psi_\mu(\vec{r}_1) \tag{A1}$$

where integration is performed over the spacial coordinates of both the neutralizing electron ($\vec{r}_1$) and the ejected electron ($\vec{r}_2$). The interaction coupling the two participating electrons is modeled by a screened Coulomb potential of the Yukawa form

$$W(\vec{r}_1 - \vec{r}_2) = \exp(-\lambda\ |\vec{r}_1-\vec{r}_2|)/(\ |\vec{r}_1-\vec{r}_2|\ ) \tag{A2}$$

where the inverse screening length associated with the metallic electron density in the vacuum region is denoted by the symbol λ. A schematic representation of the physical system is displayed in

REFERENCES (Continued)

9. J.J. Czyzewski, T.E. Madey and J.T. Yates, Jr., Phys. Rev. Lett. 32, 777(1974); T.E. Madey, J.J. Czyzewski and J.T. Yates, Jr., Surface Sci. 49, 465(1975).

10. B.J. Garrison and N. Winograd, Science, 216, 805(1982); M.L. Yu, Phys. Rev. Lett. 47, 1325(1981); M.L. Yu and N.D. Lang, Phys. Rev. Lett. 50, 127(1983); N.D. Lang, Phys. Rev. B27, 2019(1983); M.L. Yu, Phys. Rev. B26, 4731(1983).

11. J.C. Tully, Phys. Rev. B16, 4324(1977); N.H. Tolk, J.C. Tully, W. Heiland and C.W. White, Inelastic Ion-Surface Collisions (Academic, New York, 1977).

12. J.A. Applebaum and D.R. Hamann, Phys. Rev. B12, 5590(1975).

13. D. Chattarji, The Theory of Auger Transitions, (Academic Press, NY 1976).

14. J.A. Applebaum and D.R. Hamann, Phys. Rev. Lett. 32, 225 (1974).

15. S. Sawada and H. Metiu, to be published.

16. (a) F.M. Propst, Phys. Rev. 129, 7(1963);

(b) I.H. Khan, J.P. Hobson, and R.A. Armstrong, Phys. Rev. 129, 1513(1963);

(c) U. Von Gemminger, Surf. Sci. 120, 334(1982);

(d) J. Schafer, R. Schoppe, J. Holze, and R. Feder, Surf. Sci. 107, 290(1981).

REFERENCES

1. H.D. Hagstrum, Phys. Rev. 96, 336(1954); 150, 495(1966).

2. H.D. Hagstrum in Electron and Ion Spectroscopies of Solids, eds. L. Fiermans, J. Vennik and W. Kekeyser (Plenum, New York, 1978) p. 273; H. Hagstrum, J. Vac. Sci. Technol. 12, 7(1975); H. Hagstrum, Science, 178, 275(1972).

3. G.E. Becker and H.D. Hagstrum, Surf. Sci. 30, 505 (1972); H.D. Hagstrum and G.E. Becker, J. Chem. Phys. 54, 1015(1971); H.D. Hagstrum and T. Sakurai, Phys. Rev. Lett. 37, 615 (1976; T. Sakuriai and H. D. Hagstrum, Phys. Rev. B 20, 2423 (1979); H.D. Hagstrum, Phys. Rev. 104, 672(1956); H.D. Hagstrum, Phys. Rev. 123, 758(1961); H.D. Hagstrum, Phys. Rev. Lett. 43, 1050(1979); H.D. Hagstrum, Y. Takeishi, and D.D. Pretzer, Phys. Rev. 139, A526(1965); H.D. Hagstrum and Y. Takeishi, Phys. Rev. 137, A304(1965).

4. H.D. Hagstrum and G.E. Becker, Phys. Rev. B4, 4187(1971).

5. H. Conrad, G. Ertl , J. Kuppers, S.W. Wang, K. Gered and H. Haberland, Phys. Rev. Lett. 42, 1082(1979).

6. C. Boiziau, G. Garot, R. Nuvolone and J. Roussel, Surface Sci. 91, 313(1980).

7. F. Bozso, J.T. Yates, Jr., J. Arias, H. Metiu and R.M. Martin, J. Chem. Phys. 78, 4256(1983).

8. D. Menzel and R. Gomer, J. Chem. Phys. 41, 3311(1964); N. Tolk and M. Traum, eds., Desorption Induced by Electron Transitions (Springer, New York, 1982); T.E. Madey and J.T. Yates, Jr., J. Vac. Sci. Tech 8, 525(1971).

quenching spectroscopy can generate with ease IN spectra at low incident kinetic energy. The extension presented here is necessary when the orbitals of various bands have different spatial extent, so that the Auger process is controlled not only by the density of states but also by the relative orbital length scales.

It is generally true that the two electron spectroscopic methods measuring convolutions of the desired quantities are at a disadvantage when compared to their one electron competitors, since some of the details might be lost in the deconvolution process. However, if interpreted carefully IN can be a useful complement to photoelectron spectroscopy due to its extreme surface sensitivity.

ACKNOWLEDGEMENT:

This work was supported in part by the Office of Naval Research and by the National Science Foundation (CHE-83-8310106).

Most other spectra have a low energy peak.(b) The Ni 3d band has a high density of states and a short spatial extent, while the s-p band has a low density of states but extends further. This situation should cause difficulties in the Hagstrum model, but not in ours. A computation will establish how serious these difficulties are.

The parameters used in the calculation are given in Table I. Since the constant C_k, C_i, C_μ, C_ν are unknown we can only calculate the shape of the spectrum. This is not a shortcoming since the experimental measurements do not give the absolute intensities. The calculation is used to find the density of states that best fits the IN data. To do this we express the density of states as a sum of many Gaussians with unknown parameters which are varied to minimize the difference between the computed and the measured spectrum. The minimization is automated: a subroutine generating the IN spectrum, according to the method outlined in Section II, for a given set of Gaussian parameters is used in a Fletcher-Powell minimization program which varies the parameters until the best least square fit is obtained.

The best fit of the Ni(111) IN spectrum is shown in Figure 8. The discrepancy at low kinetic energy is perhaps due to the presence of secondary electrons in the experimental spectrum. In Figure 9 we show the best density of states (full line) as well as that obtained with the Hagstrum model. In Figure 10 we show a comparison between the experimental IN spectrum and a calculation using the best density of states and making the assumption that ion neutralization takes place only at the ion surface distance of $z=2.4\text{Å}$. The error introduced by this assumption is large enough to give a visibly worse fit than the full model.

IV. SUMMARY

In this paper we have developed a practical method for the analysis of ion neutralization spectra. This was stimulated by the fact that metastable

alone. The attractive part of the force is given by the image formula

$$F = (\varepsilon-1)(\varepsilon+1)\ 5.76\times10^{-20}\ qz^{-2} \qquad (19)$$

where ε is the dielectric constant of the metal, q is the ion charge and z is the ion surface distance in Å.

II. 6. Electron escape probability.

Finally, the last quantity needed for the calculation of the Auger spectrum is the escape probability $\mathcal{P}(\varepsilon_k)$, for which we use a semi-empirical formula (Equation (B.4) of Appendix B) proposed by Hagstrum, with the parameter f equal to 2.2.

III. NUMERICAL STUDIES OF THE He^+/Ni(111) SYSTEM.

We have used the model outlined in Section II to analyze the IN spectrum of the Ni(111) surface, obtained by metastable quenching spectroscopy.[7] The method probes the surface with a thermal beam of neutral He and excited (metastable) $He^*(2^1S)$ atoms. The metastable is resonantly ionized by the surface and the He^+ ion is Auger neutralized when it collides with the metal. Since resonant ionization is a long range process and Auger neutralization is a short range one we assume that we deal with a two step process: first resonant ionization, then ion neutralization. In this case the resulting IN spectrum is the same as that obtained with a low energy (~0.05 eV) ion in beam.

To compare the experimental and the computed spectra we must remove the secondary electron emission from the data. In spite of the existence of several experimental studies[16] of secondary emission, it is difficult to perform such a subtraction accurately. Because the precise shape and magnitude of the low energy part (ε_k < 5 eV) of the IN spectrum is somewhat uncertain, it was not included in our optimization calculation.

There are several reasons for choosing Ni(111) for this study: (a) its IN spectrum has a peculiar form, with a peak at high electron kinetic energy.

$\psi_i(\vec{r}) = C_i \exp(-Br)$, given in spherical coordinates with the origin of the coordinate system at the center of the ion. Since the ejected Auger electrons of interest in IN have a kinetic energy of ~13 eV or less, their De Broglie wavelength is larger than the size of the ionic orbital ψ_i which determines the integration range in Equation (16). Therefore, we can take $\psi_k(\vec{r})$ to be a constant C_k. The screened potential is taken to be of Yukawa form $W(|\vec{x}_2-\vec{x}_1|) = \exp(-\lambda|\vec{x}_2-x_1|))/(|\vec{x}_2-\vec{x}_1|)$. We have also used $W(|\vec{x}_2-\vec{x}_1|)= (|\vec{x}_2-\vec{x}_1|^{-\lambda})^{-1}$ and the results obtained with the two equations are very similar.

The calculation of the matrix element is outlined in Appendix A. The result is

$$-H(\varepsilon_k,\varepsilon_\mu,\varepsilon_\nu;z) = \frac{(2\pi)^2 C_i C_k C_\nu C_\mu}{\lambda(\alpha_\nu-\lambda)\beta(\beta-\alpha_\mu-\lambda)}\{\exp[-\beta(z-\gamma)-(\alpha_\mu+\lambda)]$$
$$[(z+\gamma) + (\beta-\alpha_\mu-\lambda)^{-1} +\beta^{-1}] \qquad (18)$$
$$-\exp[-(\alpha_\mu+\lambda)z]\ [(\beta-\alpha_\mu-\lambda)^{-1} +\beta^{-1}]\}$$

This equation is valid for $\alpha_\nu>\lambda>o$, $\beta>(\alpha_\mu-\lambda)$ and $\Delta>\gamma$ (see Appendix A). Here γ is a cut-off distance which is the ion's closest possible approach to the metal surface.

II. 5. <u>The trajectory of the incident ion</u>.

At low kinetic energy it becomes difficult to choose a proper trajectory for the ion. This is a general problem for all curve crossing models.[15] The system is simultaneously on curve one and two, with a given transition amplitude for each event. Therefore neither energy surface is providing the force alone and the total force in the correct equation of motion for the ion must depend on the gradients of the two potential energies and on the probability amplitudes describing the occupation of the two electronic states.[15] In spite of this we use here an equation of motion corresponding to the motion on the ionic surface

simplest possible model in which the orbital lengths of various bands is qualitatively incorporated.

The matrix element characterizing the Auger neutralization process is[12,13]

$$H(\varepsilon_k,\varepsilon_\nu,\varepsilon_\mu;z) = \int d\vec{r}_1 \int d\vec{r}_2\ \psi_i^*(\vec{r}_2)\ \psi_k^*(\vec{r}_1)\ W(|\vec{r}_1-\vec{r}_2|)\psi_\nu(\vec{r}_1)\psi_\mu(\vec{r}_2) \quad , \quad (16)$$

where the orbitals $\psi_i,\psi_k,\psi_\nu,\psi_\mu$ were defined above and $W(|\vec{r}_1-\vec{r}_2|)$ is a screened Coulomb interaction between two surface electrons.

Since electrons are indistinguishable particles we should subract an exchange term[13] (which is obtained by replacing $\psi_i^*(\vec{r}_2)\psi_k^*(\vec{r}_1)$ with $\psi_i^*(\vec{r}_1)\psi_k^*(\vec{r}_2)$ in Equation (16)) from the Coulomb term included in Equation (16). Previous surface Auger neutralization work,[12] which computed these matrix elements, has neglected exchange. The reason for this neglect is not clear, nor is it documented that the term is negligible. In the present context, where the main role of these matrix elements is to take into account the fact that the orbitals in different bands have different spatial extent, the inclusion of the exchange term does not seem critical.

In order to model the qualitative behavior of the matrix element $H(\varepsilon_k,\varepsilon_\nu,\varepsilon_\mu;z)$ we use the following simple forms for the orbitals. The orbitals ψ_μ and ψ_ν, describing the metal atoms are taken to be

$$\psi_\beta(\vec{r}_1) = C_\beta \exp(-\alpha_\beta z_1) \quad (17)$$

where the constants C_β and α_β have different values whether ε_β is in band A or band B. In the case of Ni the two bands are the 3d band and the s-p one. Since there are indications[1-4,12] that Auger neutralization takes place at a relatively large distance from the surface ($\sim$2Å), and that at those distances the corrugation of the electron charge density is very low,[14] we neglect the change in $\psi_\beta(\vec{r}_1)$ along the surface. The ion orbital is of the form

APPENDIX B

PROBABILITY OF ESCAPE OF AN EXCITED ELECTRON FROM A METAL SURFACE

The probability $\mathcal{P}(\varepsilon_k)$ for an excited electron of energy ε_k to escape from a metal surface is given by[1,3]

$$\mathcal{P}(\varepsilon_k) = \int_0^{2\pi} \int_0^{\theta_c} \mathcal{P}(\theta, \varepsilon_k) \sin\theta \, d\theta \, d\phi \qquad \text{(B 1)}$$

where $\theta_c(\varepsilon_k)$ is the maximum value of θ for which escape over the surface barrier is possible. Here ε_k measures the energy of the ejected Auger electron relative to the vacuum. If we assume that the angular distribution of electrons is isotropic then $\mathcal{P}(\theta, \varepsilon_k)$ is constant:

$$\mathcal{P}(\theta, \varepsilon_k) = (4\pi)^{-1} \qquad \text{(B 2)}$$

Substitution of Equation (B 2) into Equation (B 1) gives

$$\mathcal{P}(\varepsilon_k) = \left\{ \begin{array}{ll} 1-[\varepsilon_o/(\varepsilon_k+\varepsilon_o)]^{1/2}/2 & \text{for } \varepsilon_k > 0 \\ 0 & \text{for } \varepsilon_k < 0 \end{array} \right\} , \qquad \text{(B 3)}$$

where ε_o is the energy of the bottom of the conduction band with respect to vacuum. Calculations of the total electron yield using the Equation (B 3) for $\mathcal{P}(\varepsilon_k)$ give results significantly below those determined experimentally. This discrepancy between the calculated and experimentally determined total Auger electron yield suggest that $\mathcal{P}(\theta, \varepsilon_k)$ is not an isotropic function. To model the anisotropy in the Auger electron ejection pattern, the following semi-empirical expression for the electronic escape probability was developed by Hagstrum

$$\mathcal{P}(\varepsilon_k) = \begin{cases} [1 - (\varepsilon_o/(\varepsilon_k+\varepsilon_o)^{1/2}]/\{2\{1 - [1/f^2)](\varepsilon_o/(\varepsilon_k+\varepsilon_o)^{1/2}\}\}, & \varepsilon_k > 0 \\ 0 & , \varepsilon_k < 0 \end{cases} \quad \text{(B 4)}$$

The numerical value of the parameter f can be determined by fitting the calculated total Auger electron yield to experimental measurements. For helium ions incident on a clean tungsten surface with kinetic energy of 40 eV, Hagstrum gives a value of f = 2.2. Hagstrum[3] finds the value of $\mathcal{P}(\varepsilon_k)$ for $(\varepsilon_k) > 4$ eV is highly insensitive to parametric variation, so error in f do not lead to significant errors in the computed IN spectrum.

Table 1. Physical constants used for the He^+/Ni(111) system.

Helium ionization energy:

E_i (isolated atom)	24.6 eV
$E_i\ (z_m)$[(a)]	~ 22.6 eV

Exponential decay parameters:

He^+ wave function	$\beta = 3.779\ \mathring{A}^{-1}$
$\psi_i = C_i r^{-\beta r}$	

Ni(111) conduction band wave functions[(b)]:

$\psi_{4s}(z) = C_{4s} e^{-\alpha_{4s} z}$:	$\alpha_{4s} = 0.35\ \mathring{A}^{-1}$
$\psi_{3d}(z) = C_{3d} e^{-\alpha_{3d} z}$:	$\alpha_{3d} = 0.93\ \mathring{A}^{-1}$

Ni(111) conduction band energetics[(c)]:

Fermi level	$\varepsilon_F = -5.2$ eV
Lower band edge	$\varepsilon_{LBE} = -17.2$ eV

(a) Ionization energy at the position of most probable neutralization.

(b) Decay constant of atomic nickel wave functions.[26]

(c) All energies measured relative to the vacuum level.[3]

LIST OF FIGURES

1. Energy level diagram describing (a) the initial and (b) the final states in Auger neutralization of the incident ion by a metal surface. The ion is represented by the half filled ψ_i orbital. The metal orbitals ψ_μ,ψ_ν and ψ_k are involved in Auger neutralization. The ion surface distance is z.
2. Two electronic surfaces describing the energy of the ground state metal and the ion (Me + A^+), and the energy of the neutral atom A and the metal $(Me^+)^*_{\mu\nu k}$ having an electron in ψ_k and holes in ψ_μ and ψ_ν. The orbital energies are defined in Figure 1.
3. A schematic plot of the neutral curve and two ionic curves corresponding to two values of $\alpha=\varepsilon_\mu+\varepsilon_\nu$, namely, α' and α''. The ionic curves have different asymptotic energy mismatches $\Delta_{k,\alpha'}(\infty)$ and $\Delta_{k,\alpha''}(\infty)$ and different crossing possitions $Z(\alpha)$ and $Z(\alpha')$.
4. A schematic plot of the family of ionic curves labelled by various values of $\alpha \equiv \varepsilon_\mu+\varepsilon_\nu$, which can participate in Auger neutralization.
5. A schematic description of the bands A and B and the orbital ranges Z_A and Z_B discussed in the text.
6. A schematic plot of the kinetic energy ranges for the processes BB, AB, AA and BA defined in the text.
7. A schematic plot of the IN spectrum for two situations. Full line: The IN spectrum for $Z_B > Z_A$, $\varepsilon_A>\varepsilon_B$ and $\rho_B>\rho_A$ (Z_B and Z_A are defined in Figure 5, ε_A and ε_B are the orbital energies in band A and B and ρ_B and ρ_A are the density of states in the bands A and B). Broken line: The IN spectrum for $Z_A>Z_B$, $\varepsilon_A>\varepsilon_B$ and $\rho_A>\rho_B$. The AA, AB, BA and BB processes are defined in the text. The energies ε_F,ε_1, and ε_2 are defined in Figure 5. I_A and I_B are the ionization potentials of the atom at the distances Z_A and Z_B.

8. Kinetic energy distributions of electrons ejected by thermal helium ions colliding with a clean Ni(111) surface. The experimental spectrum was obtained by MQS.[7] The theoretical spectrum was computed by using the extended model described in Section II. The density of states was varied to get the best fit of the experimental IN spectrum.
9. The density of states of the Ni(111) surface. The dotted line was obtained by using the extended model and varying the density of states to produce the best fit of the experimental IN spectrum. The full line was obtained by using Hagstrum model.
10. The IN spectrum of the Ni(111) surface, computed by using the "best density of states" shown in Figure 9 and by assuming that the neutralization of the ion takes place at $z = 2.4$ Å.
11. The coordinate system and the notation used for the evaluation of the matrix elements.

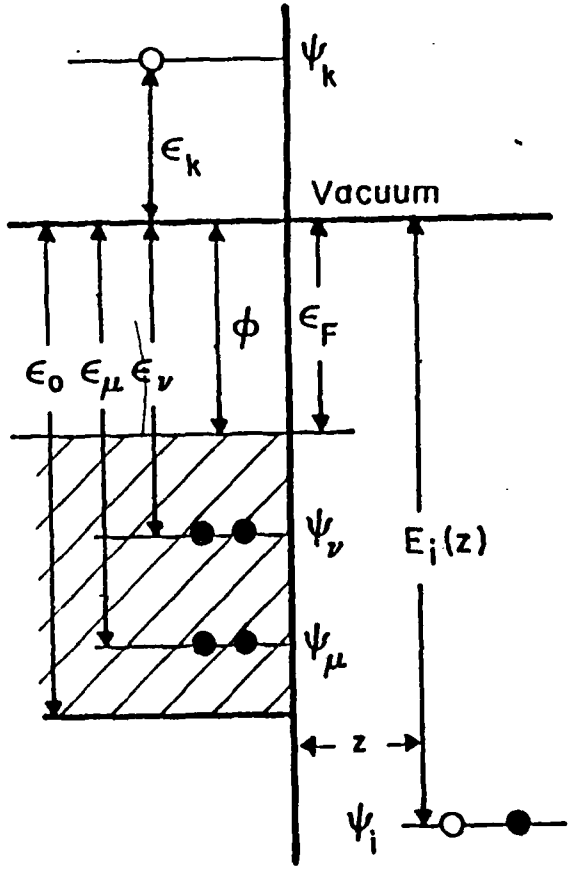
ψ_k
ϵ_k
Vacuum
ϵ_0 ϵ_μ ϵ_ν
ϕ
ϵ_F
ψ_ν
$E_i(z)$
ψ_μ
z
ψ_i
Metal
Ion

(a)

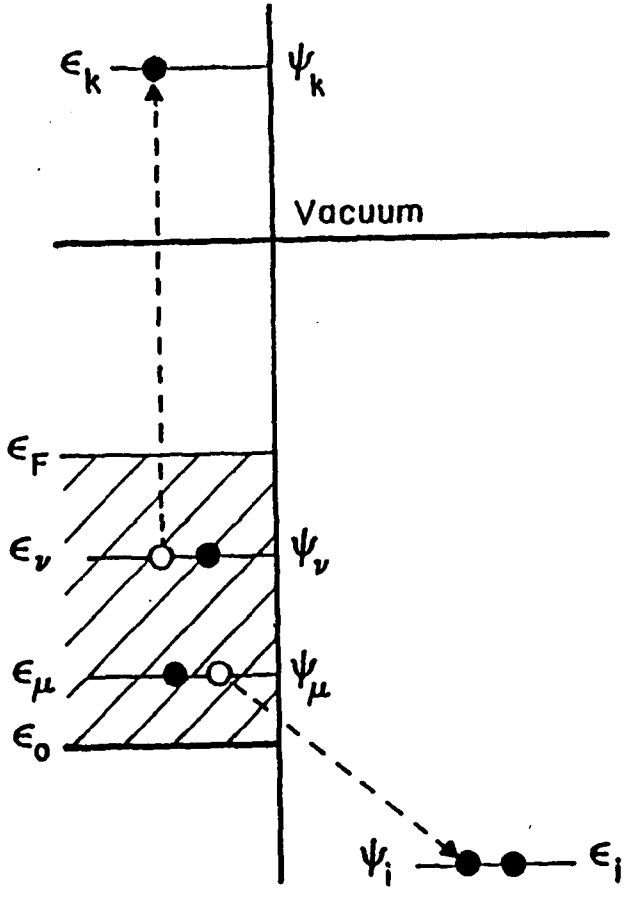
ϵ_k
ψ_k
Vacuum
ϵ_F
ϵ_ν
ψ_ν
ϵ_μ
ψ_μ
ϵ_0
ψ_i
ϵ_i
Metal$^+$
Neutral

(b)

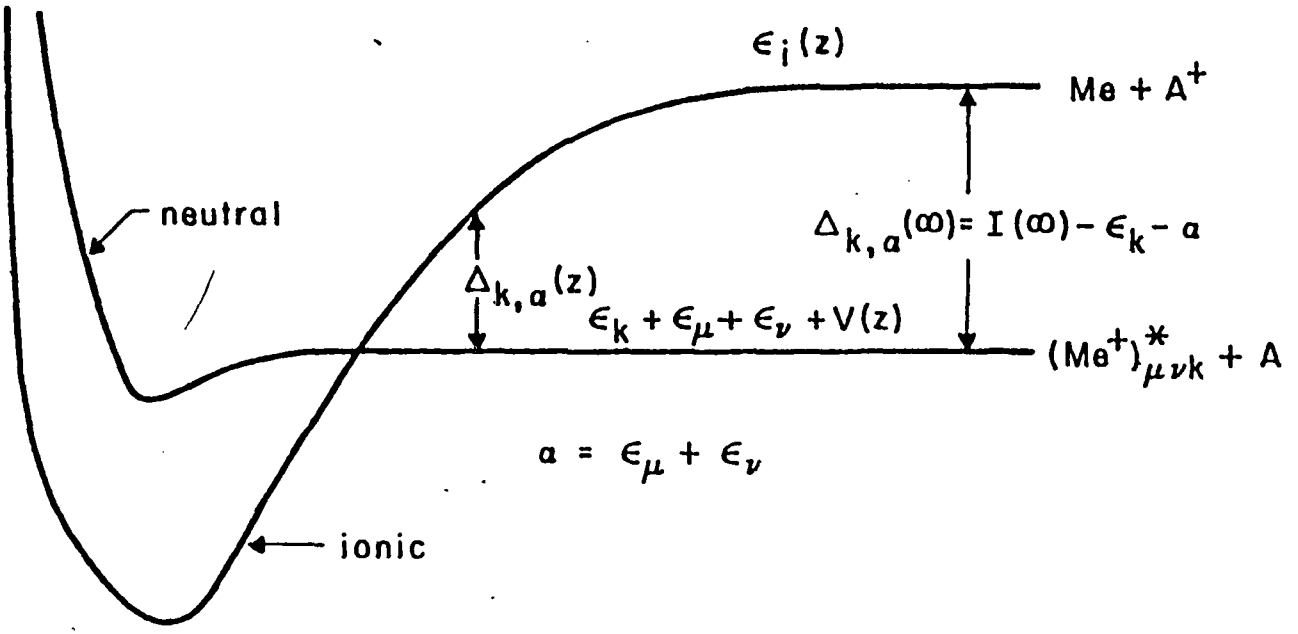
$\epsilon_i(z)$
Me + A^+
neutral
$\Delta_{k,a}(\infty) = I(\infty) - \epsilon_k - a$
$\Delta_{k,a}(z)$
$\epsilon_k + \epsilon_\mu + \epsilon_\nu + V(z)$
$(Me^+)^*_{\mu\nu k}$ + A
$a = \epsilon_\mu + \epsilon_\nu$
ionic

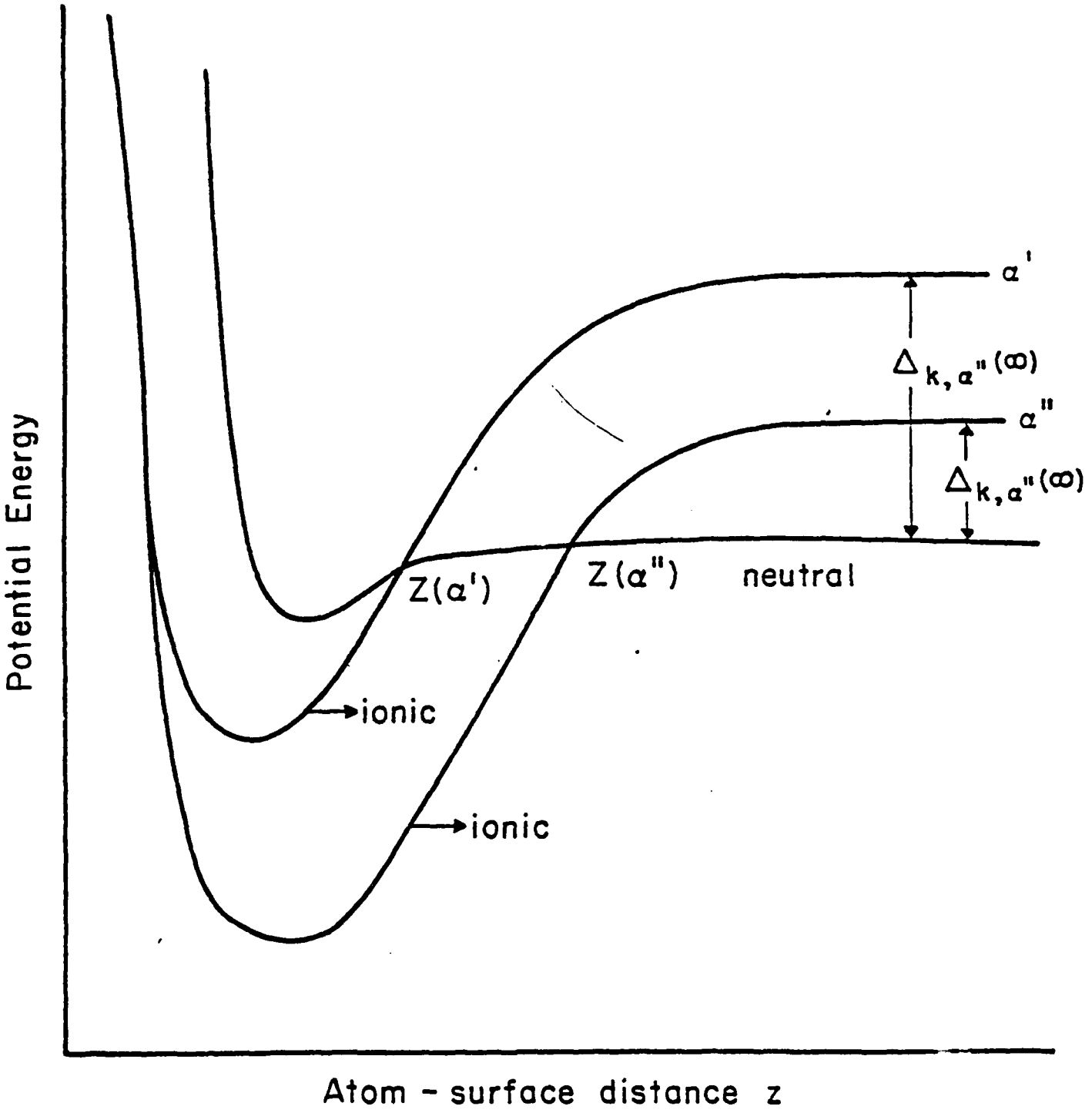
Potential Energy
α'
Δ k, α" (∞)
α"
Δ k, α" (∞)
Z(α')
Z(α")
neutral
ionic
ionic
Atom - surface distance z

Fig. 3

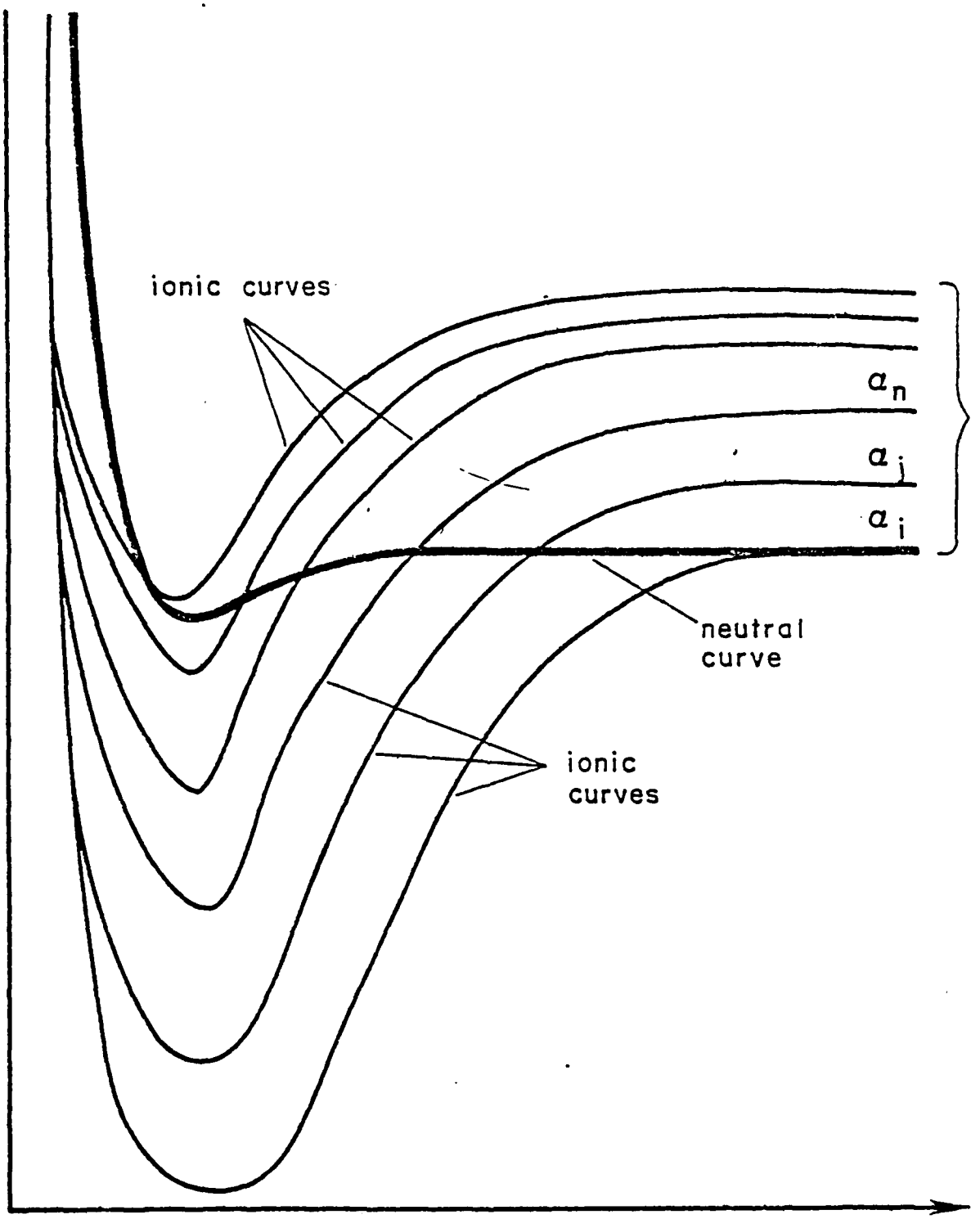
ionic curves
α_n
α_j
α_i
neutral curve
ionic curves

Fig. 4

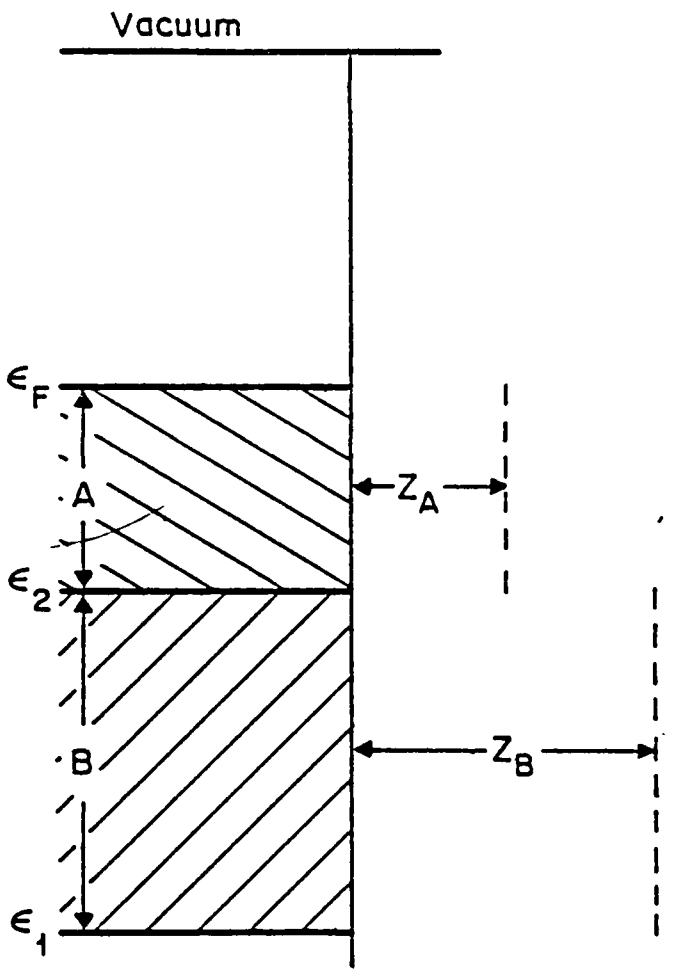

Fig. 5

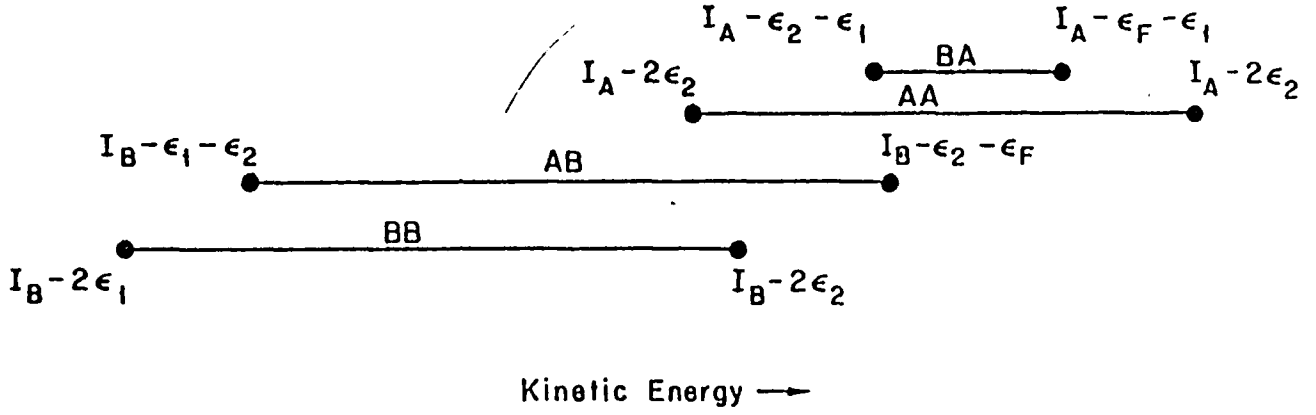
$I_A - \epsilon_2 - \epsilon_1$
$I_A - \epsilon_F - \epsilon_1$
BA
$I_A - 2\epsilon_2$
AA
$I_A - 2\epsilon_2$
$I_B - \epsilon_1 - \epsilon_2$
AB
$I_B - \epsilon_2 - \epsilon_F$
BB
$I_B - 2\epsilon_1$
$I_B - 2\epsilon_2$
Kinetic Energy →

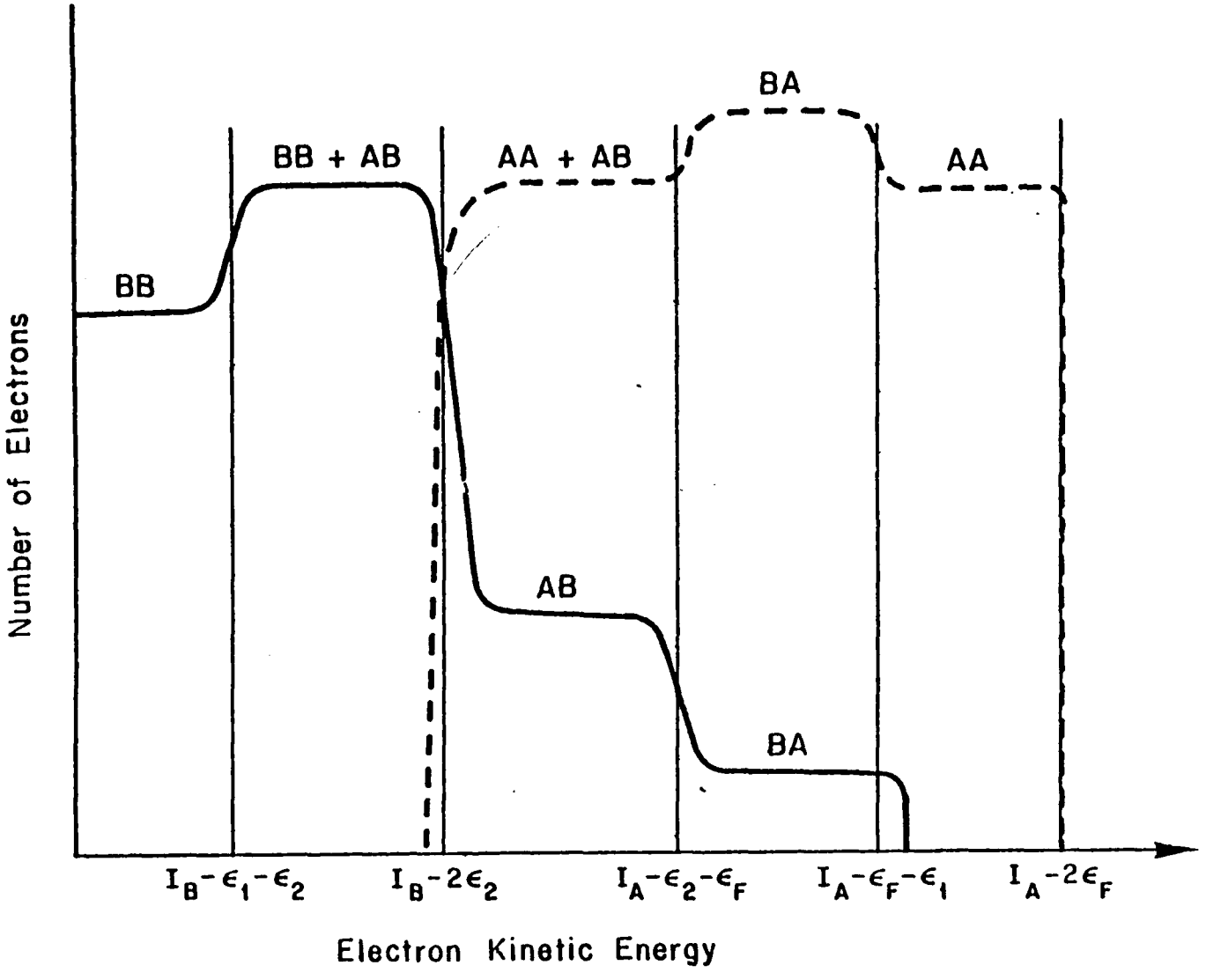
BA
BB + AB
AA + AB
AA
BB
AB
BA
Number of Electrons
$I_B-\epsilon_1-\epsilon_2$
$I_B-2\epsilon_2$
$I_A-\epsilon_2-\epsilon_F$
$I_A-\epsilon_F-\epsilon_1$
$I_A-2\epsilon_F$
Electron Kinetic Energy

Fig. 7

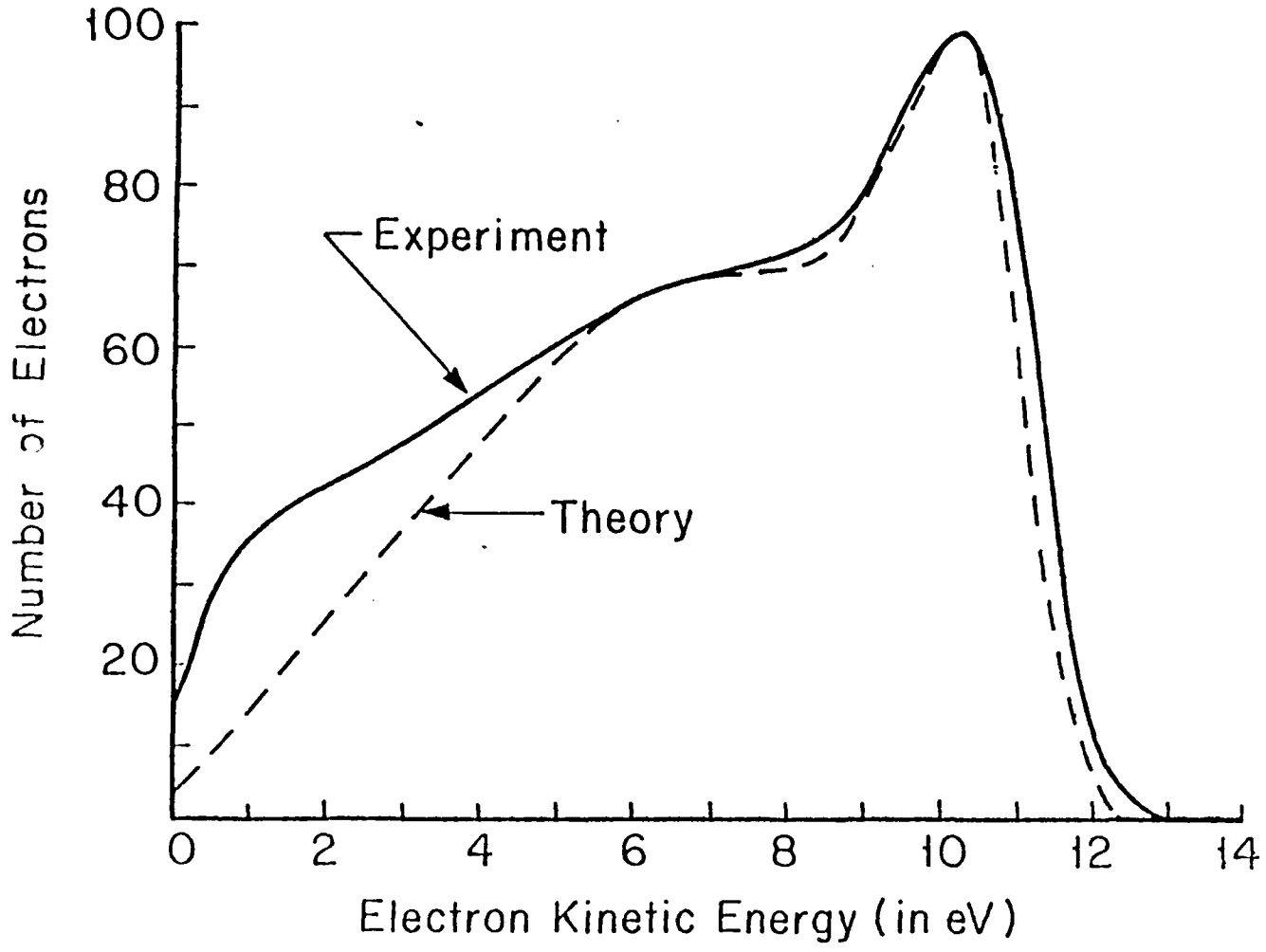
100
80
60
40
20
Number of Electrons
Experiment
Theory
0
2
4
6
8
10
12
14
Electron Kinetic Energy (in eV)

ig. 8

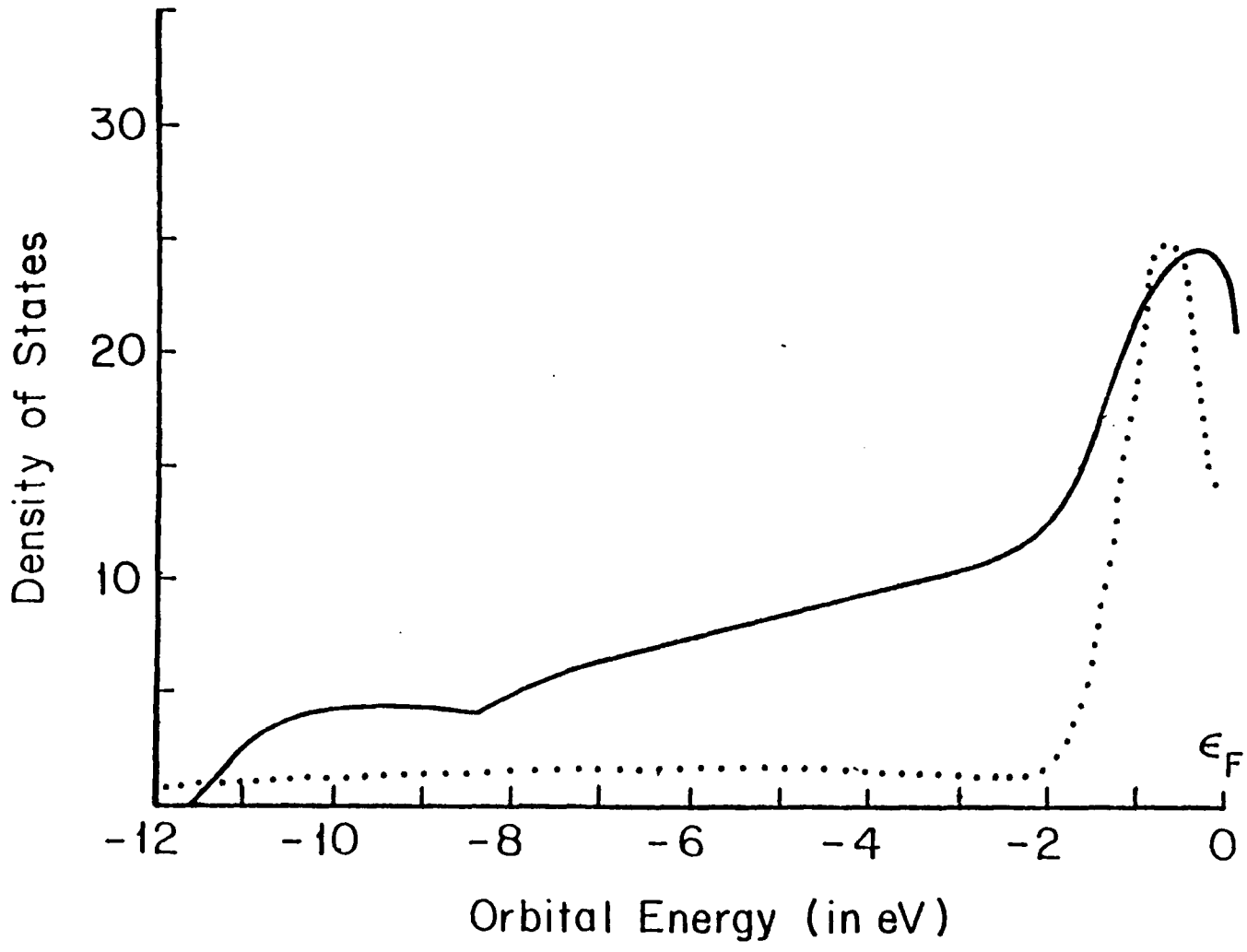
Density of States
30
20
10
ϵ_F
-12
-10
-8
-6
-4
-2
0
Orbital Energy (in eV)

Fig. 9

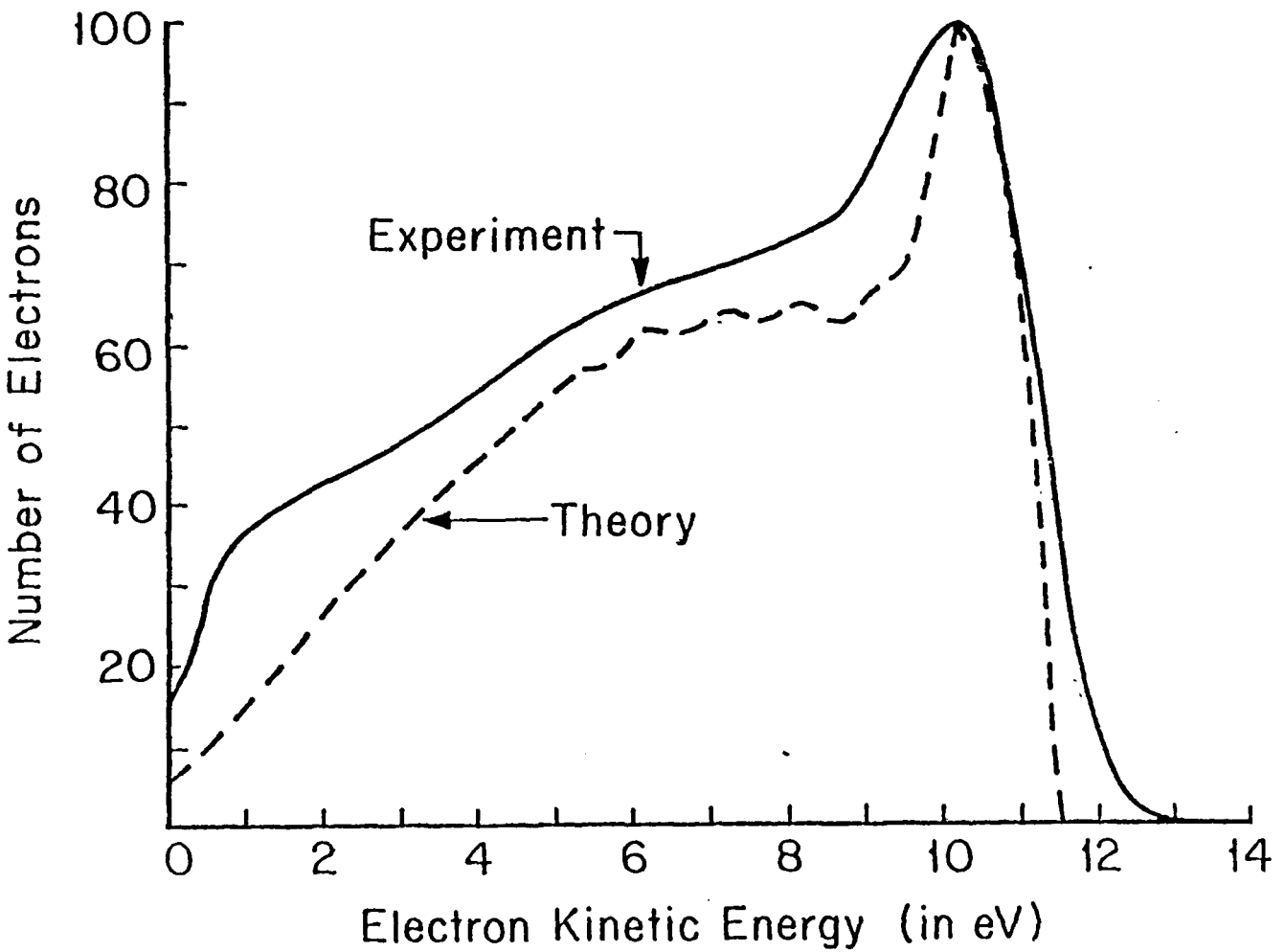
100
80
60
40
20
Number of Electrons
Experiment
Theory
0
2
4
6
8
10
12
14
Electron Kinetic Energy (in eV)

Fig. 10

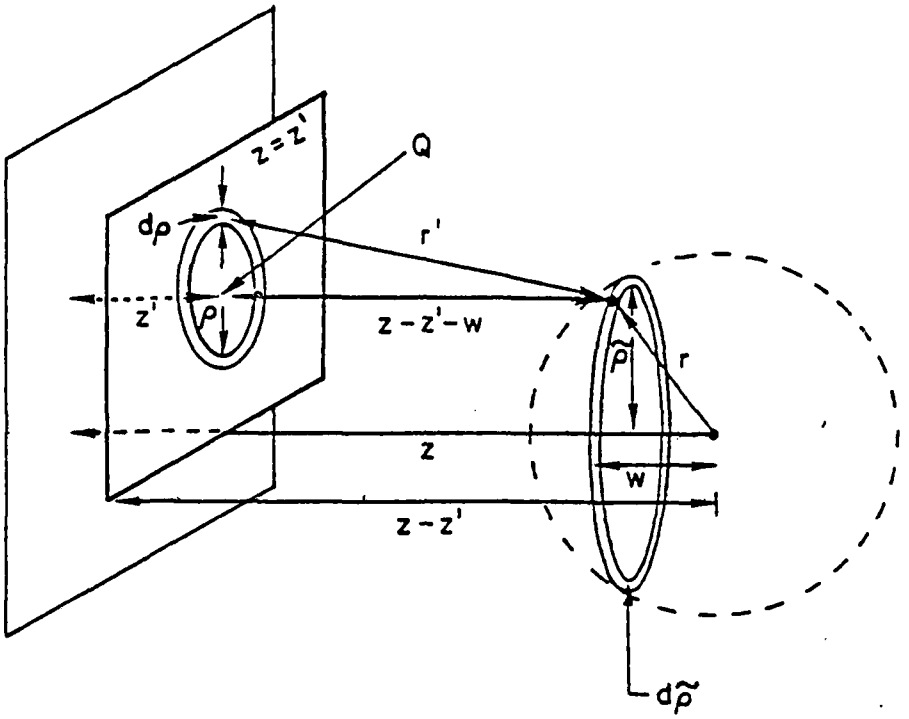
z=z'
Q
dρ
r'
z'
ρ
z-z'-w
ρ̃
r
z
w
z-z'
dρ̃

END

FILMED

5-85

DTIC